Langmuir
Article
pubs.acs.org/Langmuir

Structure of Micelles Formed by Highly Asymmetric Polystyrene-*b*-Polydimethylsiloxane and Polystyrene-*b*-poly[5-(*N*,*N*-diethylamino)isoprene] Diblock Copolymers

Fernando C. Giacomelli,[†] Izabel C. Riegel,[‡] Petr Stepánek,[§] Cesar L. Petzhold,[⊥] Mario D. Ninago,[⊥] Ángel J. Satti,[⊥] Andrés E. Ciolino,[⊥] Marcelo A. Villar,[⊥] Vanessa Schmidt,[¶] and Cristiano Giacomelli*[,¶]

[†]*Centro de Ciências Naturais, Universidade Federal do ABC, 09210-170 Santo André, Brazil,* [‡]*Departamento de Química, Universidade Federal do Paraná, 81531-990, Curitiba, PR, Brazil,* [§]*Institute of Macromolecular Chemistry, Heyrovsky Sq. 2, 162 06 Prague 6, Czech Republic,* [⊥]*Instituto de Química, Universidade Federal do Rio Grande do Sul, 91501-970 Porto Alegre, Brazil,* [⊥]*Planta Piloto de Engeniéria Química, 8000, Bahía Blanca, Argentina, and* [¶]*Departamento de Química, Universidade Federal de Santa Maria, 97105-900, Santa Maria, Brazil*

Received June 15, 2010. Revised Manuscript Received August 4, 2010

The internal structure of polystyrene(PS)-shell micelles having core-forming blocks consisting of polydimethylsiloxane (PDMS) or poly[5-(*N*,*N*-diethylamino)isoprene] (PAI) was determined in detail by accessing the multilevel structural organization using static and dynamic light scattering and small-angle X-ray scattering techniques. Well-defined PS-*b*-PDMS and PS-*b*-PAI diblock copolymers with molar masses in the range of 12.0k−18.2k g/mol were dispersed in cyclohexane, dimethylacetamide, or dimethylformamide. Colloidal nanoparticles exhibiting either swollen core with a large surface area per corona chain that enables the PS chains to assume a random coil conformation with Gaussian statistics, or compact core and slightly stretched PS chains in the corona were obtained. Therefore, the results of this study provide an interesting alternative allowing for precise control of the core and corona properties of PS-*b*-PDMS and PS-*b*-PAI micelles in selective solvents. Admittedly, such differences in terms of micellar properties can dictate the potential of block copolymer micelles for generating thin films from preformed nano-objects, as well as the capability to function as nanoreactors in organic medium.

Introduction

The production of complex multifunctional soft-matter nanostructures with tunable stability and behavior is certainly among the next major challenges in the rapidly expanding field of macromolecular sefl-assembly.[1] As a bottom-up process, molecular level characteristics of elementary building blocks (chemical nature of blocks, composition, length, and architecture) are obviously key design parameters, which can be tailored through clever application of recent advances in controlled/living polymerization techniques.[2−11] Such a versatility may also be advantageously extended by manipulating the interactions between polymer−polymer chains and polymer−solvent during the process of preparation of association colloids. The formation of block copolymer micelles is a result of the complex balance of two main opposing forces.[5] The first driving force corresponds to the attraction between the insoluble blocks and is related to the high interfacial energy between solvent and insoluble chains that induces the aggregation and, consequently, the reduction in the free energy of the polymer chains. The second one refers to the repulsion between the soluble blocks that limits the size of the aggregates and provokes the extension of polymer chains hence increasing the elastic free energy of the system.[5,12] Experimentally, this thermodynamic balance may be altered by changing the Flory−Huggins interaction parameter (χ) between the solvent and core-forming block by wisely choosing the selective solvent as well as by modifying the size and/or nature of the block-forming chains.[3,5,8−12] As a result, the structural characteristics of the micelles such as number of aggregation, critical micellar concentration, hydrodynamic radius, core and shell dimensions, and the conformation of polymer chains will certainly change as well. In highly solvent-sensitive systems, morphological transitions from spherical to cylindrical micelles to vesicles can be attained by controlling the Flory−Huggins interaction parameter between polymer chains and solvents.[13]

The polystyrene-*block*-polydimethylsiloxane (PS-*b*-PDMS)[14] copolymer belongs to the class of polymer systems exhibiting an intrinsic high χ-value (i.e., highly incompatible segments—χ is estimated to be four times higher than for polystyrene-*b*-polyisoprene)[15,16] that usually helps in achieving long-range order

*To whom correspondence should be addressed. E-mail: cgiacomelli@pq.cnpq.br.

(1) Ober, C. K.; Cheng, S. Z. D.; Hammond, P. T.; Muthukumar, M.; Reichmanis, E.; Wooley, K. L.; Lodge, T. P. *Macromolecules* **2009**, *42*, 465.
(2) Giacomelli, C.; Schmidt, V.; Aissou, K.; Borsali, R. *Langmuir*, published online April 5, **2010**, http://dx.doi.org/10.1021/la100641j.
(3) Lazzari, M.; Liu, G.; Lecommandoux, S. *Block Copolymers in Nanoscience*; Wiley-VCH Verlag GmbH & Co.: Darmstadt Germany, 2006.
(4) Ikkala, O.; Brinke, G. *Chem. Commun*. **2004**, 2131.
(5) Hamley, I. W. *Block Copolymers in Solution: Fundamentals and Applications*; Wiley: New York, 2005.
(6) Lodge, T. P.; Pudil, B.; Hanley, K. J. *Macromolecules* **2002**, *35*, 4707.
(7) Discher, B. M.; Hammer, D. A.; Bates, F. S.; Discher, D. E. *Curr. Opin. Colloid Interface Sci*. **2000**, *5*, 125.
(8) Allen, C.; Maysinger, D.; Eisenberg, A. *Colloid Surf. B* **1999**, *16*, 3.
(9) Riess, G. *Prog. Polym. Sci*. **2003**, *28*, 1107.
(10) Bucknall, D. G.; Anderson, H. L. *Science* **2003**, *302*, 1904.
(11) Bates, F. S.; Fredrickson, G. H. *Annu. Rev. Phys. Chem*. **1990**, *41*, 525.
(12) Duxin, N.; Eisenberg, A. Transmission Electron Microscopy Imaging of Block Copolymer Aggregates in Solutions. In *Soft-Matter Characterization*, Pecora, R., Borsali, R., Eds.; Springer: New York, 2008.
(13) Uneyama, T. *J. Chem. Phys*. **2007**, *126*, 114902.
(14) Ninago, M. D.; Ciolino, A. E.; Villar, M. A.; Giacomelli, F. C.; Cernoch, P.; Stepánek, P.; Schmidt, V.; Giacomelli, C. *Chem. Eng. Trans*. **2009**, *17*, 1807.

Table 1. Macromolecular Characteristics of the Diblock Copolymers Used in This Study

entry	copolymer[a]	M_n (g/mol)[b]	M_w/M_n	w_{PS}[c]
1	PS_{171}-*b*-$PDMS_6$	18200	1.04	0.97
2	PS_{117}-*b*-$PDMS_{44}$	15400	1.09	0.79
3	PS_{82}-*b*-$PDMS_{62}$	13200	1.09	0.65
4	PS_{147}-*b*-PAI_6	13600	1.20	0.95
5	PS_{132}-*b*-PAI_8	14000	1.06	0.93
6	PS_{126}-*b*-PAI_{10}	12000	1.20	0.90

[a] Subscripts refer to the mean degree of polymerization determined using M_w and the weight fraction of PAI or PDMS. [b] Determined by SEC measurements. [c] Weight fraction of PS in the block copolymer.

during the production of thin films for soft nanolithography.[17] This diblock is also attractive for applications relying on nanopattern transfer due to the presence of a Si-rich etch-resistant segment.[17] Comparatively, polystyrene-*block*-poly[5-(*N*,*N*-diethylamino)isoprene] (PS-*b*-PAI)[18,19] should also follow the same trend in terms of compatibility, despite the lack of precise information available at this stage. Regarding the systems mentioned above, it was verified previously that both PDMS and PAI homopolymers are not soluble in dimethylacetamide (DMAc) and dimethylformamide (DMF) which are, on the other hand, selective solvents for the PS block. On the contrary, all the blocks that constitute the copolymers (PDMS, PAI, and PS) are soluble in cyclohexane (CH). Therefore, micellar nano-objects having PDMS or PAI cores stabilized by a solvent-philic PS-shell originate upon self-assembly of PS-*b*-PDMS and PS-*b*-PAI diblocks in DMAc and DMF. The internal structure of micelles prepared from the former has not yet been probed by techniques allowing direct measurements at such a scale, as indeed accessible by small-angle X-ray scattering (SAXS). Similar association colloids were investigated by Aliferis and Iatrou[20] who determined the influence of the polymer architecture (linear vs miktoarm stars) on the aggregation phenomena by means of static and dynamic light scattering techniques. Micelles having comparable core−shell architecture and composition may also be obtained in 1,2-dichlorobenzene/benzyl alcohol,[21] whereas reverse aggregates may be prepared in *n*-heptane or *n*-dodecane.[22] Exploring such possibilities in an effort to fabricate surfaces with ultrahydrophobicity, Ning et al.[22] described a method for controlling the surface chemical composition and topography of films obtained from PS-*b*-PDMS diblock copolymer by casting copolymer solutions from solvents with different selectivity.

In the present study, we determined the structure of polystyrene-shell micelles having different core-forming blocks for two polymer systems—PS-*b*-PDMS[14] and PS-*b*-PAI[18]—in solvents of different selectivity, using small-angle X-ray scattering (SAXS) and static and dynamic light scattering (SLS and DLS) techniques. Insights into the relationship between the macromolecular characteristics and the conformation of the chains in the micellar structure (core and shell) are provided by accessing multilevel structural organization and by associating such data with polymer−polymer and polymer−solvent interaction parameters.

Experimental Section

Samples and Solutions. The synthesis and characterization of polystyrene-*block*-polydimethylsiloxane (PS_x-*b*-$PDMS_y$) and polystyrene-*block*-poly[5-(*N*,*N*-diethylamino)isoprene] (PS_x-*b*-PAI_y) diblock copolymers (here and throughout the text subscripts *x* and *y* refer to the mean degree of polymerization) used in this study have been recently described.[14,23,24] The respective macromolecular characteristics are summarized in Table 1. Micellar solutions were prepared by applying the direct dissolution method, which consists in dissolving the polymers in pure DMF, DMAc, or cyclohexane. The resulting solutions were stirred gently at room temperature overnight before increasing the temperature to 50 °C for about 12 h. In selected cases, the formation of micelles could be identified by visual inspection due to the typical bluish aspect (Tyndall effect). Finally, the samples were filtered using 0.45 μm pore-size membrane filters in order to remove dust and any large, nonmicellar aggregates. The solvents employed for solutions preparation (DMF, $n = 1.430$, $\eta = 0.92$ cP; DMAc, $n = 1.438$, $\eta = 1.93$ cP; and cyclohexane, $n = 1.426$, $\eta = 0.89$ cP; with n being the refractive index and η being the viscosity at 293 K)[25] were of analytical grade (Aldrich) and used as received.

Measurements and Data Analysis. *Static and Dynamic Light Scattering (SDLS).* SDLS measurements were performed using an ALV CGE laser goniometer, which consists of a 22 mW HeNe linear polarized laser operating at a wavelength of 632.8 nm, an ALV 6010 correlator, and a pair of avalanche photodiodes operating in the pseudo-cross-correlation mode. The copolymer solutions were placed in 10 mm diameter glass cells and maintained at a constant temperature of 20 ± 1 °C in all experiments. The minimum sample volume required for DLS experiments was 1 mL. Data were collected using ALV Correlator Control software and the counting time varied for each sample from 300 to 900 s.

Static light scattering (SLS) measurements were carried out varying the scattering angle (θ) from 30 to 150° with a 15° stepwise increase. Decalin was used as a calibration standard. The mass-average molar mass (M_w), *z*-average radius of gyration (R_g), and second virial coefficient (A_2) values were estimated using the formalism of Zimm as described in detail elsewhere.[19] In the dynamic light scattering (DLS) mode, the measured intensity correlation functions $g_2(t)$ were analyzed using the algorithm REPES (incorporated in the GENDIST program) which employs the inverse Laplace transformation according to $g_2(t) - 1 = \beta[\int A(\tau)\exp(-t/\tau)\,d\tau]$, where t is the delay time of the correlation function and β is an instrumental parameter.[26] The resulting $A(\tau)$ function is a distribution of relaxation times consisting generally of several peaks representing individual dynamic processes. Herein, the distributions of relaxation times are shown in the equal area representation as $\tau A(\tau)$ vs $\log \tau$.[27] The relaxation frequency, Γ ($\Gamma = \tau^{-1}$) depends generally on the scattering angle, and in the case of a diffusive particle, this frequency is q^2-dependent.[28] Consequently, the apparent diffusion coefficient (D_{app}) at a given copolymer concentration (c) was calculated from $\Gamma/q^2|_{q\to 0} = D_{app}$, where q is the wavevector defined as $q = 4\pi n/\lambda \sin(\theta/2)$, with λ being the wavelength of the incident laser beam and θ being the scattering angle. The hydrodynamic radius (R_H) (or diameter, $2R_H$) was calculated from the Stokes−Einstein relation $R_H = k_B T/(6\pi\eta D_{app})$, where k_B is the Boltzmann constant, T is the temperature of the sample, and η is the viscosity of the solvent.

(15) Krause, S.; Iskandar, M.; Iqbal, M. *Macromolecules* **1982**, *15*, 105.
(16) Chu, J. H.; Rangarajan, P.; Adams, J. L.; Register, R. A. *Polymer* **1995**, *36*, 1569.
(17) Jung, Y. S.; Ross, C. A. *Nano Lett.* **2007**, *7*, 2046.
(18) Giacomelli, F. C.; Riegel, I. C.; Petzhold, C. L.; Silveira, N. P.; Stepanek, P. *Langmuir* **2009**, *25*, 3487.
(19) Giacomelli, F. C.; Riegel, I. C.; Petzhold, C. L.; da Silveira, N. P.; Stepanek, P. *Langmuir* **2009**, *25*, 731.
(20) Aliferis, T.; Iatrou, H. *Eur. Polym. J.* **2008**, *44*, 2412.
(21) Fukumine, Y.; Inomata, K.; Takano, A.; Nose, T. *Polymer* **2000**, *41*, 5367.
(22) Ning, Z.; Xiaoyan, Z.; Xiaoli, Z.; Jian, X. *ChemPhysChem* **2007**, *8*, 1108.
(23) Petzhold, C. L.; Stadler, R. *Macromol. Chem. Phys.* **1995**, *196*, 2625.
(24) Petzhold, C. L.; Kolshorn, H.; Stadler, R. *Macromol. Chem. Phys.* **1995**, *196*, 1405.
(25) *Handbook of Chemistry and Physics*; Lide, D. R., Ed.; CRC Press: Boca Raton, FL, 2004.
(26) Jakes, J. *Collect. Czech. Chem. Commun.* **1995**, *60*, 1781.
(27) Stepánek, P. In *Dynamic Light Scattering: The Method and Some Applications*; Brown, W., Ed.; Oxford Science Publications: Oxford, 1993.
(28) Brown, W. *Dynamic Light Scattering. The Method and Some Applications*; Oxford University Press Inc.: New York, 1993.

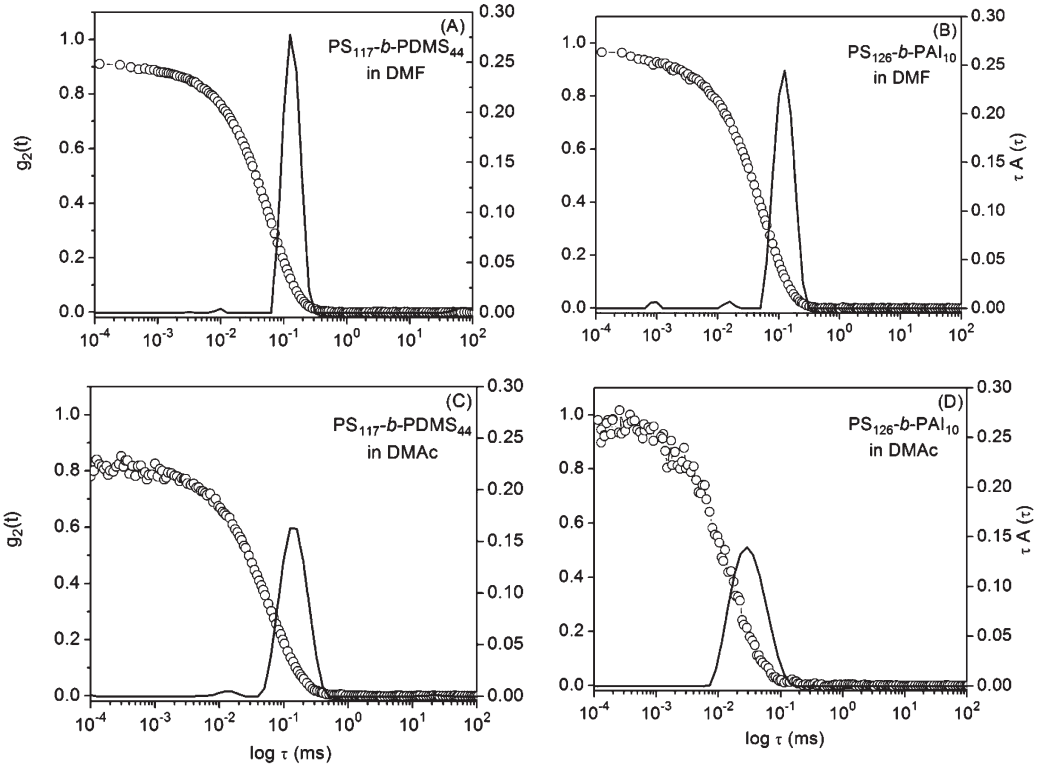

Figure 1. Autocorrelation functions $g2(t)$ measured at a scattering angle 90° (symbols) and distributions of the relaxation times $\tau A(\tau)$ at 90° as revealed by REPES algorithm (solid lines) for solutions containing PS_{117}-*b*-$PDMS_{44}$ (left) and PS_{126}-*b*-PAI_{10} (right) dissolved in DMF (top) and DMAc (bottom) at $c = 5$ mg/mL.

Small Angle X-ray Scattering (*SAXS*). SAXS experiments were performed at the D11A-SAXS beamline of the Brazilian Synchrotron Light Laboratory (LNLS−Campinas, SP, Brazil). Block copolymer solutions were loaded in a temperature controlled vacuum flow-through cell composed of two mica windows separated by 2 mm, normal to the beam.[29] The collimated beam crossed the sample through an evacuated flight tube and was scattered to a 2D CCD marCCD detector with active area of 16 cm^2. The 2D scattering patterns were collected after an exposure time of 600 s. To cover the desired q range (from 0.07 to 1.70 nm^{-1}) where $n \approx 1$ for X-rays, the sample-to-detector distance was set to 2019.4 mm (silver behenate was used for sample-to-detector distance calibration). In all cases, the 2D-images were found to be isotropic, and they were corrected by taking into account the detector dark noise and normalized by the sample transmission considering the 360° azimuthal scan. The above procedure was undertaken using the FIT2D software developed by A. Hammersley.[30] Furthermore, the resulting $I(q)$ vs q scattering curves were corrected by the subtraction of the scattering of the pure solvent and further placed on an absolute scale using water as standard. The sample and solvent scattering can be measured at the same conditions allowing a very reliable background subtraction. The $I(q)$ vs q scattering profile of the block copolymer micelles could be fitted using the spherical copolymer micelle model developed by Pedersen and Gerstenberg.[31] A summary of the model can be found in the following section. The fitting procedures and other analyses were performed using the SASfit software, which makes use of the least-squares fitting approach for minimizing the squared chi (χ^2) parameter. The SASfit software package was developed by J. Kohlbrecher, and it is available free of charge.[32]

Results and Discussion

The macromolecular characteristics of the PS-*b*-PDMS and PS-*b*-PAI diblock copolymers used in this study are summarized in Table 1. The polymer chains were found to have a low dispersity in terms of size ($M_w/M_n \leq 1.20$), in agreement with conventional living anionic polymerization protocols. These polymers are, therefore, very convenient model systems for self-assembling studies as long as the well-known dispersity effects of the building blocks are minimized. The micellar solutions investigated hereinafter were prepared by the direct dissolution method.[8,9] The formation of so-called hairy or starlike micelles (radius of the nucleus $R_c \ll$ corona width W) is anticipated in the present case due to the high weight fraction of solvent-philic PS block ($w_{PS} \geq 0.65$).[33]

SDLS experiments were carried out prior to SAXS measurements in order to first determine the dimensional properties of scattering nano-objects found in solutions containing PS-*b*-PDMS and PS-*b*-PAI chains dissolved in three different solvents. Then, the detailed internal structure of the nano-objects was evaluated by SAXS.

Light Scattering Measurements. Figure 1 shows typical autocorrelation functions and distributions of the relaxation times for solutions containing PS_{117}-*b*-$PDMS_{44}$ and PS_{126}-*b*-PAI_{10} diblock copolymers in DMF and DMAc. In all the cases, reasonably narrow distributions of relaxation times were obtained with a dominant mode corresponding to the diffusive motion of the particles in solution, as characterized by the q^2-dependence of the relaxation frequency.[28] Such particles are very

(29) Cavalcanti, L. P.; Torriani, I. L.; Plivelic, T. S.; Oliveira, C. L. P.; Kellermann, G.; Neuenschwander, R. *Rev. Sci. Instrum.* **2004**, *75*, 4541.
(30) Hammersley, A. P. Scientific software FIT2D; http://www.esrf.eu/computing/scientific/FIT2D/ (accessed July 28, 2009).
(31) Pedersen, J. S.; Gerstenberg, M. C. *Macromolecules* **1996**, *29*, 1363.
(32) Kohlbrecher, J. *Software package SASfit for fitting small-angle scattering curves*, http://kur.web.psi.ch/sans1/SANSSoft/sasfit.html: 2009.
(33) Daoud, M.; Cotton, J. P. *J. Phys.-Paris* **1982**, *43*, 531.

Table 2. Physical−Chemical Properties of Scattering Nano-objects Determined by SDLS Measurements[a]

entry	copolymer	$\langle r \rangle$ (nm)	R_H (nm)	μ_2/Γ^{2a}	$M_{w(micelle)}$ ($\times 10^5$ g/mol)	N_{agg}	scattering object
			Solvent = Cyclohexane				
1-CH	PS_{171}-*b*-$PDMS_6$	8.9	3.1				unimer
2-CH	PS_{117}-*b*-$PDMS_{44}$	8.5	2.9				unimer
3-CH	PS_{82}-*b*-$PDMS_{62}$	8.0	2.8				unimer
4-CH	PS_{147}-*b*-PAI_6	8.3	2.8				unimer
5-CH	PS_{132}-*b*-PAI_8	7.9	2.6				unimer
6-CH	PS_{126}-*b*-PAI_{10}	7.8	2.6				unimer
			Solvent = DMAc				
1-Ac	PS_{171}-*b*-$PDMS_6$	8.9	10.0	0.11	1.7	09	micelle
2-Ac	PS_{117}-*b*-$PDMS_{44}$	8.5	9.8	0.12	2.6	17	micelle
3-Ac	PS_{82}-*b*-$PDMS_{62}$	8.0	8.9	0.13	3.2	25	micelle
4-Ac	PS_{147}-*b*-PAI_6	8.3	2.3				unimer
5-Ac	PS_{132}-*b*-PAI_8	7.9	2.0				unimer
6-Ac	PS_{126}-*b*-PAI_{10}	7.8	1.9				unimer
			Solvent = DMF				
1-F	PS_{171}-*b*-$PDMS_6$	8.9	16.2	0.13	2.5	14	micelle
2-F	PS_{117}-*b*-$PDMS_{44}$	8.5	15.5	0.14	4.5	29	micelle
3-F	PS_{82}-*b*-$PDMS_{62}$	8.0	14.9	0.12	5.6	43	micelle
4-F	PS_{147}-*b*-PAI_6	8.3	2.3				unimer
5-F	PS_{132}-*b*-PAI_8	7.9	14.2	0.12	2.9	19	micelle
6-F	PS_{126}-*b*-PAI_{10}	7.8	13.6	0.11	3.2	22	micelle

[a] Dispersity estimated by cumulant analysis of the autocorrelation functions recorded at 90° scattering angle.

uniform in terms of size as judged from the low dispersity values calculated using the cumulant analysis ($\mu_2/\Gamma^2 < 0.15$). Therefore, nano-objects having well-defined dimensions exist in solution in any case. This is a very important feature which indeed validates the SLS technique for accessing unambiguously the mass-average molar mass of micelles ($M_{w,mic}$).

The physical-chemical properties of organic solutions containing PS-*b*-PDMS and PS-*b*-PAI diblock copolymers, as determined by SDLS measurements, are summarized in Table 2. The data obtained in cyclohexane revealed that none of the samples formed micellar aggregates. In fact, the experimental D_H values ($D_H = 2R_H$) were found to be in agreement with the theoretical average unperturbed end-to-end distance $\langle r \rangle$ of a polymer chain. The value of $\langle r \rangle$ is given by $\langle r \rangle = b\sqrt{N}$, where b is the statistical segment length ($b_{PS} = 0.67$ nm)[34] and N is the number of repeating units.[35] Noting that the amount of polymer in solution is well-below the theoretical critical overlap polymer concentration (c^*),[36] the observation above suggests that molecularly dissolved chains (unimers) are present in solution in those cases. As such, they produce very low scattered light intensity in SLS measurements (data not shown), and originate SAXS profiles that can be reasonably described by the Debye function (see below). Therefore, these experimental results confirm that the PS-*b*-PDMS and PS-*b*-PAI samples investigated in this work do not generate association colloids in cyclohexane, which can thus be considered a good solvent for all polymer segments. It is worth noting that cyclohexane at 34.5 °C is a theta solvent for PS (main component of the diblocks), thus implying that PS−cyclohexane interactions are virtually absent (or at least very weak) under the experimental conditions of this study.[37] Hence, the conformation of PS chains should be almost ideal with Gaussian statistics.

In DMAc medium, the PS-*b*-PAI copolymers still dissolved molecularly (D_H ($=2R_H$) $\approx \langle r \rangle$, Table 2) in spite of the significantly different solubility parameter in such a case as compared to the hydrocarbon environment (see Supporting Information Table S2 for solubility parameters of solvents and homopolymers). The relatively short PAI segment may be either soluble in the medium or stabilized by the much longer solvent-philic PS block. Interestingly, the R_H values of unimers in cyclohexane were slightly larger than in the other solvents, most likely because in the latter case PS chains are forced to contract because of unfavorable polymer−solvent interactions.

In contrast, the size of the scattering objects made from PS-*b*-PDMS diblocks in DMAc is out of the range acceptable for single chains, clearly suggesting that such a system self-organizes to originate micellar aggregates. Nonetheless, it is worth noting that REPES analysis revealed the presence of a relaxation mode faster than that associated with micellar aggregates in this case, although with very small amplitudes (Figure 1A,C). This fast mode can be attributed to the diffusion of free copolymer chains in equilibrium with aggregates. Indeed, a small number of free chains is detectable in light scattering measurements depending on the criteria for data analysis, even if they produce low scattered light intensity owing to their much lower mass as compared to the micelles. In addition, small contributions sometimes revealed by the REPES analysis in the very fast region are related to motions of the solvent molecules, as deeply discussed elsewhere.[38]

The comparison of results for PS_{171}-*b*-$PDMS_6$ and PS_{147}-*b*-PAI_6 in DMAc (entries 1-Ac and 4-Ac in Table 2, respectively), highlights substantial differences between the two block copolymer systems. For the same degree of polymerization of the core-forming block, the PDMS-containing diblock exhibited self-assembly ability, while the PAI counterpart did not. We believe that this is explained in a qualitative sense on the basis of the Flory−Huggins polymer−solvent interaction parameter ($\chi_{polymer-solvent}$), which depends on the solubility parameter (δ) of

(34) Zhao, W.; Zhao, X.; Rafailovich, M. H.; Sokolov, J.; Composto, R. J.; Smith, S. D.; Satkowski, M.; Russel, T. P.; Dozier, W. D.; Mansfield, T. *Macromolecules* **1993**, *26*, 561.
(35) Hiemenz, P. C. *Polymer Chemistry: The Basic Concepts*; Marcel Dekker: New York, 1984.
(36) Teraoka, I. *Polymer Solutions: An Introduction to Physical Properties*; Wiley: New York, 2002.
(37) Higgins, J. S.; Benoit, H. C. *Polymers and Neutron Scattering*; Clarendon Press: Oxford, 1994.
(38) Stepanek, P.; Tuzar, Z.; Kadlec, P.; Kriz, J. *Macromolecules* **2007**, *40*, 2165.

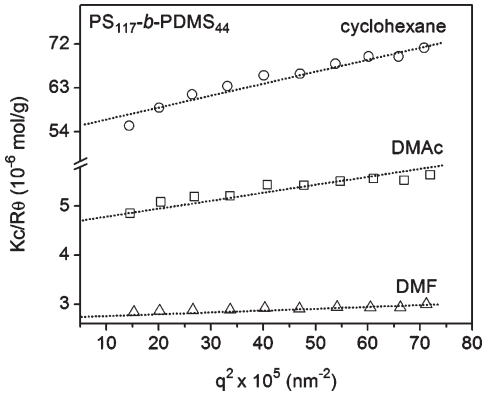

Figure 2. Partial Zimm plots for 5 mg/mL PS_{117}-*b*-$PDMS_{44}$ diblock copolymer solutions in DMF, DMAc, and cyclohexane, as indicated.

the interacting pair according to $(\delta_{polymer} - \delta_{solvent})^2$. While the value of δ for PAI is unfortunately not available in the literature to the best of our knowledge, we note that δ for unmodified PI ($\delta_{(PI)} = 15.8$) is higher than for PDMS ($\delta_{(PDMS)} = 15.1$) (Supporting Information, Table S2). Taking into account the molecular structure of PAI, we speculate that $\delta_{(PAI)} > \delta_{(PDMS)}$ and consequently $\chi_{PAI\text{-}DMAc} < \chi_{PDMS\text{-}DMAc}$. The higher degree of incompatibility between PDMS segment and DMAc solvent is, consequently, at the origin of its ability to self-assemble into micelles in DMAc. In doing this analysis, it should be noted that in most polymer−solvent systems there is a large (even dominant) entropy contribution that is impossible to predict a priori. The estimates of solubility parameters can be used only in a most qualitative sense as above.

The results in Table 2 also reveal that, regardless of the block copolymer composition, molar mass and soluble block weight fraction, the size of the self-assembled nano-objects is practically the same (R_H = 8.9−10.0 nm). In fact, this is only possible if the thermodynamics associated with the formation of micellar aggregates changes since the number and conformation of unimers having different lengths must obviously be different in order to generate particles of the same size, as effectively corroborated by SAXS. While essentially the same comments also apply for PS-*b*-PDMS micelles in DMF, the micellar size measured in such a solvent ($R_H \approx 15$ nm) was found to be approximately 50% larger than in DMAc ($R_H \approx 10$ nm). Curiously, PS-*b*-PAI micelles were barely smaller than PS-*b*-PDMS analogues, although their core-forming blocks are much shorter (see for instance entries 2-F and 5-F, Table 2).

The above-mentioned particles were found to be isotropic according depolarized light scattering measurements. Experiments performed after positioning a Glann−Thompson prism with extinction ratio better than 10^{-7} before the entrance of the light scattered detector (the correct position of the prism was verified using the well-known depolarization ratio of benzene (I_{VH}/I_{VV} = 0.26) as standard) did not detect depolarized light scattering contributions from micellar solutions. This result suggests the absence of anisotropic scattering objects such as cylinders and ellipsoids. Details on the internal structure of above-mentioned nanoparticles will be discussed hereafter using complementary SLS and SAXS experiments.

The mass-average molar mass ($M_{w,mic}$) and aggregation number (N_{agg}) of micelles was determined by SLS using the Zimm formalism. Figure 2 shows typical partial Zimm plots for 5.0 mg/mL PS_{117}-*b*-$PDMS_{44}$ diblock copolymer solutions prepared using different solvents, as indicated. We note that in these experiments the scattered light intensity is proportional to $(dn/dc)^2$, and n_{PDMS} = 1.41 which means that PDMS is nearly isorefractive with DMF and DMAc. Accordingly, the M_w extracted from data shown in Figure 2 should refer exclusively to the PS component of either unimers or micelles. On the other hand, PAI is isorefractive with toluene as observed experimentally, hence suggesting that $n_{PAI} \approx 1.50$. Taking into account such information, the accurate $M_{w(micelle)}$ for PS-*b*-PDMS micellar aggregates in DMF and DMAc can be calculated according to eq 1,

$$M_{w(micelle)} = \frac{M_{w(PS)}}{w_{PS}} \quad (1)$$

where $M_{w(PS)}$ is the experimental value obtained from the SLS. The molar mass of micelles ($M_{w(micelle)}$) and the molar mass of the respective individual diblock copolymer chains ($M_{w(unimer)}$) are related according to eq 2, from which the micelle aggregation number (N_{agg}) is accessible.[39] The values thus calculated (Table 2) revealed that the absolute number of chains per PS-*b*-PDMS micelle is higher in DMF than in DMAc due to the fact that $\chi_{PDMS\text{-}DMF} > \chi_{PDMS\text{-}DMAc}$, while in both solvents N_{agg} generally increases with the increase in the solvophobic block length (or weight fraction of thereof). Essentially the same comments can also be extended to the PS-*b*-PAI system in DMF.

$$N_{agg} = \frac{M_{w(micelle)}}{M_{w(unimers)}} \quad (2)$$

While it is well-known that the aggregation number is defined by a set of multifaceted contributions that possibly includes the strongest influence coming from the length of the insoluble polymer segment, it should also scale with the degree of polymerization (DP) of the soluble block as given by eq 3 in the case of starlike micelles (i.e., N_{agg} is expected to decrease as the length of the corona-forming block increases). In the present study, therefore, N_{agg} is also dictated by the length of the core-forming block.

$$N_{agg} \approx \left(\frac{1}{\ln(DP_{PS})}\right)^{6/5} \quad (3)$$

SAXS Measurements. The internal structure of the block copolymer micelles already identified above was investigated by SAXS. The scattering intensity $I(q)$ of an isotropic solution of monodisperse particles embedded in a matrix with a constant electron density, after normalization with the background scattering of the solvent, is given by

$$I(q) = NP(q)\,S(q) \quad (4)$$

wherein N is the number of scattering particles per unit volume, $P(q)$ is the form factor of an individual particle, and $S(q)$ is the structure factor arising from long-range correlations between scattering centers. For widely separated systems as is the case of solutions with low copolymer content, $S(q) \approx 1$, and $I(q)$ consequently represents the form factor $P(q)$ that reflects size and shape of the scattering objects.

Figure 3 shows representative SAXS patterns for PS_{117}-*b*-$PDMS_{44}$ and PS_{126}-*b*-PAI_{10} diblock copolymers in DMF and DMAc at c = 20 mg/mL. At a glance, the high X-ray scattering intensity in the low-q range of panels A−C in Figure 3 suggested the existence of association colloids, whereas in the case of panel

(39) Mountrichas, G.; Mpiri, M.; Pispas, S. *Macromolecules* **2005**, *38*, 940.

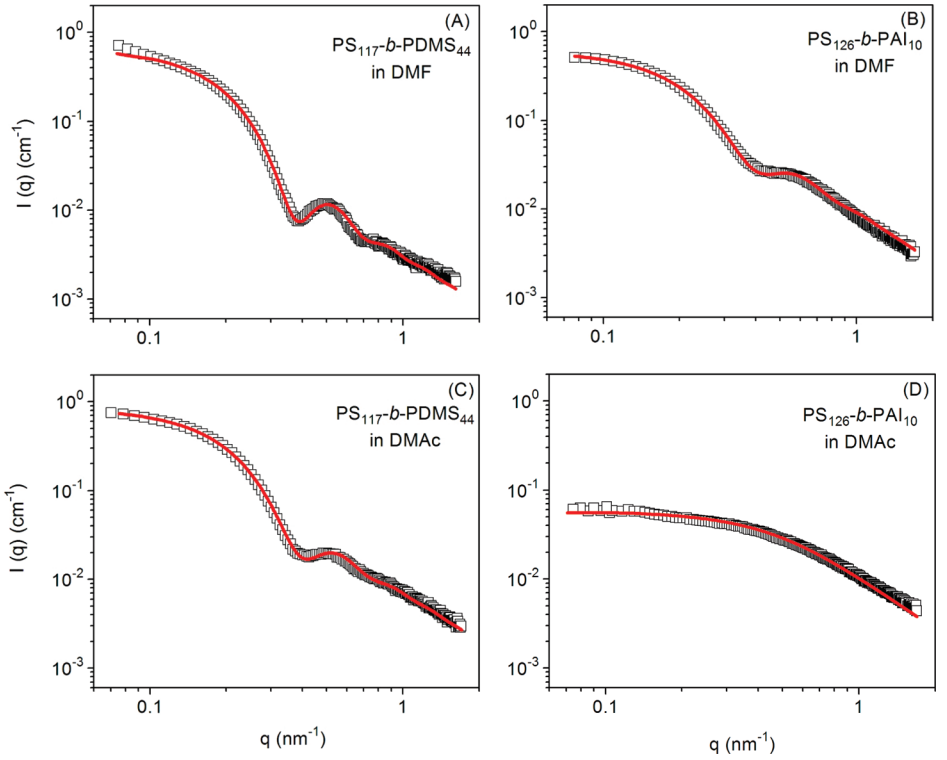

Figure 3. Experimental SAXS data (symbols) and respective curve fittings for spherical copolymer micelle or free chains model (lines) for solutions containing PS_{117}-*b*-$PDMS_{44}$ (left) and PS_{126}-*b*-PAI_{10} (right) dissolved in DMF (top) and DMAc (bottom) at $c = 20$ mg/mL.

D in Figure 3 there basically appeared a plateau at the small angle region, followed by a reduction in scattering intensity in the high-q range, which is indicative of molecularly dissolved chains (free chains or unimers). As expected, SAXS patterns, typical of free chains, were also found for all the diblock copolymer samples that did not form self-organized structures, as previously pointed out in Table 2. In such cases, the q^{-a} slope in the high-q range (Porod regime) reveals important information about the chains statistics,[37] namely, $a = -2$ for Gaussian chains (polymers in a theta solvent), $a \approx -1.67$ for chains with excluded volume (polymer in a good solvent), and $a = -1$ for rigid rodlike chains. In general, the Porod slope values (a) determined for copolymer chains in cyclohexane were found to decrease progressively from -1.54 toward -1.85 as the relative amount of PS in the copolymer increased (data not shown). Such a tendency of a to approach -2 confirmed that cyclohexane is a relatively better solvent for PAI and PDMS than for PS. In fact, this is reasonable since cyclohexane is a theta solvent for PS at 34.5 °C,[37] one should expect $a = -2$ for such a conformation.

The high-q range profile for self-assembled nanoparticles is dominated by the "*blob*" scattering from PS chains anchored to the micellar cores of PDMS or PAI. This is so because the scattering contrast between PDMS or PAI and DMF is much lower than that between PS and DMF. Indeed, the SAXS profiles could be satisfactorily fitted only using the so-called spherical copolymer micelle model formerly developed by Pedersen and Gerstenberg,[31] and revisited recently.[40] Such a model describes the scattering for micelles consisting of a homogeneous spherical core having corona chains that follow Gaussian statistics attached to the surface of the core, as depicted in Figure 4. The model does not prevent the chains from penetrating into the core region, but this can be limited by displacing the starting point of the Gaussian chains. The fact that this model adequately fit the experimental data is already remarkable since the micellar structures herein investigated consist of weakly scattering cores.

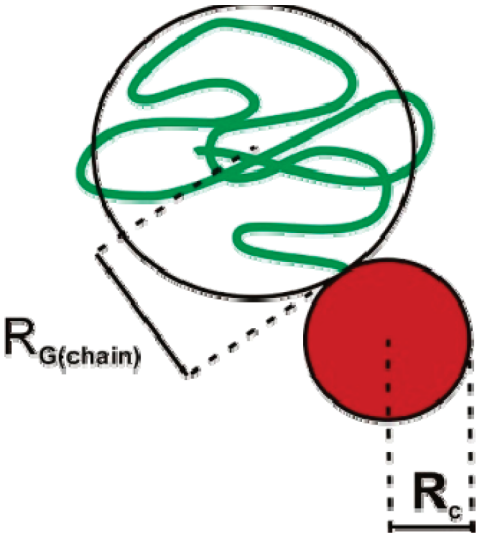

Figure 4. Schematic representation for the micellar form factor analysis according to the spherical copolymer micelle model, which consists of a spherical core of radius R_c surrounded by Gaussian chains with radius of gyration R_G attached to it.

The micellar form factor $P_{mic}(q)$ is the sum of four different terms comprising the self-correlation of the core, $F_{core}(q,R_c)$; the self-correlation term of the polymer chain inside the corona, $F_{chain}(q,R_G)$; the cross term between core and chains, $S_{core\text{-}chain}(q)$; and the cross term between different chains inside the corona,

(40) Pedersen, J. S. Small-Angle Scattering from Surfactants and Block Copolymer Micelles. In *Soft-Matter Characterization*; Borsali, R.; Pecora, R., Eds.; Springer: New York, 2008.

Table 3. Physical−Chemical Properties of Scattering Nano-Objects Determined by SAXS Measurements

entry	copolymer	R_c (nm)	R_G (nm)	R_{mic} (nm)	N_{agg}	Porod slope	β_{core} (10^{-12} cm)	β_{chain} (10^{-10} cm)	$R_{c(th)}$ (nm)	A_c (nm^2)	$\sigma N^{1.2}$
						Solvent = DMAc					
1-Ac	PS_{171}-*b*-$PDMS_6$	3.7	3.6	10.9	10	−1.60			1.3	17.2	1.7
2-Ac	PS_{117}-*b*-$PDMS_{44}$	5.4	2.6	10.6	16	−1.60			2.9	22.9	0.8
3-Ac	PS_{82}-*b*-$PDMS_{62}$	5.6	2.5	10.6	25	−1.62			3.6	15.7	0.8
						Solvent = DMF					
1-F	PS_{171}-*b*-$PDMS_6$	2.1	4.9	11.9	12	−1.40	0.76	2.26	1.4	4.6	4.2
2-F	PS_{117}-*b*-$PDMS_{44}$	4.9	3.4	11.7	39	−1.45	5.58	1.54	3.7	7.7	2.5
3-F	PS_{82}-*b*-$PDMS_{62}$	5.9	2.6	11.1	54	−1.65	7.87	1.08	4.8	8.0	1.5
4-F	PS_{147}-*b*-PAI_6										
5-F	PS_{132}-*b*-PAI_8	1.9	4.0	9.9	11	−2.01	−4.14	1.68	1.8	4.1	5.3
6-F	PS_{126}-*b*-PAI_{10}	4.5	2.8	10.1	18	−1.99	−5.18	1.60	2.3	11.7	1.7

$S_{chain-chain}(q)$. $P_{mic}(q)$ can thus be expressed as

$$P_{mic}(q) = N_{agg}^2\beta_{core}^2F_{core}(q,R_c) + N_{agg}^2\beta_{chain}^2F_{chain}(q,R_G) + N_{agg}(N_{agg}-1)\beta_{chain}^2S_{chain-chain}(q) + 2N_{agg}^2\beta_{chain}\beta_{core}S_{core-chain}(q) \quad (5)$$

where N_{agg} is the aggregation number of the micelles, and β_{core} and β_{chain} account for the excess scattering length density of the core-forming (PAI or PDMS) and corona-forming block (PS), respectively. The expressions of cross terms, core−chain and chain−chain in eq 5 depend on the geometry of the core, and they are given in ref 40 and literature cited therein.

This model has a large number of fitting parameters, namely, R_G, d, R_c, N_{agg}, and the excess scattering length density of the core and corona forming blocks (β_{core} and β_{chain}). Therefore, it is usually not possible to get a single set of fitting parameters if β_{core} and β_{chain} are not preset, and generally the fittings provide ambiguous results. Hence, during the fitting procedures the parameters β_{core} and β_{chain} were held fixed. The values of β (β_{core} and β_{chain}) for different block copolymers were calculated in the following way:

$$\beta_{core} = N_xV_x(\sigma_x - \sigma_{solvent}) \quad (6)$$

where N_x is the degree of polymerization of the polymer segment, V_x is the volume of one monomer unit, σ_x is the scattering length density of the polymer segment, and σ_{solv} is the scattering length density of the solvent. The volume occupied by a single monomer unit V_x was determined taking into account the homopolymer density d_x according to the relation:

$$V_x = \frac{M_x}{d_xN_A} \quad (7)$$

Then, the value of scattering length density of the solvents and monomer units was calculated using the average chemical composition of each component and its mass density (d_x) as

$$\sigma_x = \frac{b_ed_xN_A}{M_x}\sum_i n_iz_i \quad (8)$$

where N_A is the Avogadro's number, n_i accounts for the number of atoms i in each component, and z_i is the atomic number of the atom i (n_iz_i is the number of electrons in each unit). Finally, b_e is the Thomson scattering length (the scattering length of an electron, $b_e = 2.817 \times 10^{-13}$ cm). All the parameters thus calculated are given in Table S3 (Supporting Information).

The experimental curve fitting parameters were, therefore, N_{agg}, d, R_c, and R_G. The parameter associated with the dispersity of the particles was not included in the analysis of SAXS patterns because the DLS data already confirmed the narrow size distribution of the nano-objects. In Figure 3, the solid red lines correspond to the best fittings using the spherical copolymer micelle model. The high quality of the fittings can be straightforwardly noticed, and indeed attested by χ^{2-} values which remained below 1.65, thus corroborating that such a model can properly reproduce the whole experimental curves. Still, we have observed that in some cases the high-q region was not fitted to the same degree of accuracy, which is understandable since the model predicts a q^{-2} scattering dependence at the high-q region for describing noninteracting Gaussian chains attached to the core.

In all the cases, it can be seen that the experimental points lie above the theoretical solid red curve, which means that $a > -2$, thus implying that PS chains at the micellar corona are in a slightly different conformation as compared to a random coil with Gaussian statistics. In fact, the PS chains must assume a relatively more stretched conformation in order to give $a < -2$. The parameters extracted from the SAXS curve fittings and the actual Porod slopes of the curves in the high-q region are given in Table 3.

The core radius (R_c) was found to increase with the increase in the solvophobic block length for all copolymer and solvent systems studied in this work. Such a behavior mirrors the variation of N_{agg} determined by partial Zimm plots, hence suggesting that the size of the micellar core is not only due to a longer core-forming segment, but also due to a larger number of chains in the core.

At this stage, it is meaningful to compare the experimental R_c values with the theoretical ones $R_{c(th)}$ that would be observed for completely dry cores (in the absence of solvent). $R_{c(th)}$ can be estimated from the volume occupied by the amount of material forming the core according to the relation:

$$R_{c(th)} = \left(\frac{3N_{agg}M_wwt_{core-block}}{4\pi N_Ad_{core-block}}\right)^{1/3} \quad (9)$$

This calculation revealed that the nuclei of PS-*b*-PDMS and PS-*b*-PAI micelles may not be conceptually compact, and are most likely a bit swollen by residual solvent molecules, as attested by the fact that in general $R_{c(th)} < R_c$. Indeed, the difference becomes more accentuated when using DMAc as solvent which is more likely to remain entrapped within cores since it is a better dispersion medium for the core-forming block than DMF. The difference is however fully acceptable, and so is the use of the spherical block copolymer micelles model justified in the analysis

of SAXS curves. Importantly, it is practically impossible to estimate the degree of swelling by the change in the core scattering contrast considering that β_{chain} is roughly 2 orders of magnitude higher than β_{core} (data not shown), and $\sigma_{PDMS} \sim \sigma_{DMAc}$, and that is the reason for the fact that even though β_{core} and β_{chain} were fixed during the fitting procedures, we could achieve very good agreement between the experimental and theoretical curves.

Since R_c and N_{agg} were found to be a function of the macromolecular characteristics and solvent system, the core surface area available per chain in micellar corona (A_c) and the chain conformation itself should also depend on such physical chemical variables. Unless other mechanisms that define the conformation of polymer chains are present, the smaller the area available on the core surface is, the more stretched configuration the chains will assume. This feature can be accessed, at least qualitatively, through the factor $\sigma N^{1.2}$ formerly adopted by Eisenberg et al.,[41,42] where σ is a dimensionless parameter defined as $\sigma = l^2/A_c$, with l being the length of a repeat unit ($l_{(PS)} = 0.25$ nm[39]). In such an approach, macromolecular chains adopting stretched conformations should result in $\sigma N^{1.2} > 1$. Indeed, this is observed in Table 3. In DMF, PS-*b*-PDMS micelles are formed by a PS corona in which the chains are extended. According to the high-q range Porod slopes, the degree of stretching of the PS chains follow the order PS_{171}-*b*-$PDMS_6$ > PS_{117}-*b*-$PDMS_{44}$ > PS_{82}-*b*-$PDMS_{62}$, and PS_{132}-*b*-PAI_8 > PS_{126}-*b*-PAI_{10}. On the other hand, in DMAc the corona chains are more relaxed owing the smaller Flory−Huggins interaction parameter of PS with DMAc as compared to DMF. In addition, the higher compatibility between PDMS and DMAc in relation to DMF leads to micellar nanoparticles with rather swollen cores (already discussed above), therefore increasing the accessible core surface area per chain.

Conclusions

The self-assembly behavior of PS-*b*-PDMS and PS-*b*-PAI diblock copolymer systems was investigated in three different dispersion media (cyclohexane, DMAc, and DMF), in which self-organized structures consisting of PDMS or PAI solvophobic cores surrounded by a stabilizing interface of PS chains can be obtained in same cases. The characteristics of the thermodynamically stable micellar aggregates are strictly related to the Flory−Huggins interaction parameter (χ) between the core-forming block and the solvent, as well as to the core-forming block length. While in cyclohexane slight modifications in terms of chain statistics are observed, none of the diblock undergoes association due to the limited degree of incompatibility between the components (low $\chi_{PDMS\text{-}cyclohexane}$ and $\chi_{PAI\text{-}cyclohexane}$ values). However, this scenario evolves considerably when DMAc is chosen as solvent. The high solubility parameter of the latter resulted in an increase in the $\chi_{PDMS\text{-}DMAc}$ to an extent that was sufficient to induce the formation of self-assembled nanoparticles. Such particles, however, possess a swollen core and consequently a larger core surface area per corona chain, which allows the PS chains to assume a random coil conformation with Gaussian statistics. Owing to the low volume fraction of the core-forming segment, the PS-*b*-PAI samples used in this study remain as single chains in DMAc. In contrast, whenever PS-*b*-PAI samples were dissolved in DMF which has a higher solubility parameter than DMAc, just two monomer units are enough to change the self-assembly properties of the system. Specifically, while the PS_{147}-*b*-PAI_6 copolymer is molecularly dissolved in DMAc, the two-aminoisoprene-unit longer PS_{132}-*b*-PAI_8 formed well-defined spherical micelles in DMF. In such a solvent, PS-*b*-PDMS micelles having a compact core and slightly stretched PS chains in the corona were obtained. Our results above provide interesting alternatives to precisely control the core properties of PS-*b*-PDMS and PS-*b*-PAI micelles. This is admittedly an important step forward, mainly in the case of PS-*b*-PAI micelles, which have been used as nanoreactors to synthesize sterically stabilized gold nanoparticles in organic medium in one-pot single-step processes. In these applications, the characteristics of the nanoreactor (micelle core) may define several properties of the particles.

Acknowledgment. The authors acknowledge financial support from CONICET and ANPCyT/Argentina (PICT 22-38462), Grant Agency of the Czech Republic (202/09/2078), and CNPq/Brazil (Grant No. 476703/2008-5).

Supporting Information Available: Physical−chemical properties of block copolymers, solvents, and their respective solutions. This material is available free of charge via the Internet at http://pubs.acs.org.

(41) Zhang, L.; Eisenberg, A. *J. Am. Chem. Soc.* **1996**, *118*, 3168.
(42) Zhang, L. F.; Barlow, R. J.; Eisenberg, A. *Macromolecules* **1995**, *28*, 6055.